PROCEEDINGS B

royalsocietypublishing.org/journal/rspb

Research

**Cite this article:** Souquet L, Guenser P, Girard C, Mazza M, Rigo M, Goudemand N. 2022 Temperature-driven heterochrony as a main evolutionary response to climate changes in conodonts. *Proc. R. Soc. B* **289**: 20220614. https://doi.org/10.1098/rspb.2022.0614

Received: 31 March 2022
Accepted: 27 September 2022

**Subject Category:**
Evolution

**Subject Areas:**
palaeontology, evolution

**Keywords:**
developmental bias, environment, evolution, conodonts, geometric morphometrics, macroevolution

**Authors for correspondence:**
Louise Souquet
e-mail: louise.souquet@gmail.com
Nicolas Goudemand
e-mail: nicolas.goudemand@ens-lyon.fr

†Present address: Department of Mechanical Engineering, University College London, London, UK.

Electronic supplementary material is available online at https://doi.org/10.6084/m9.figshare.c.6238496.

THE ROYAL SOCIETY PUBLISHING

# Temperature-driven heterochrony as a main evolutionary response to climate changes in conodonts

Louise Souquet[1,†], Pauline Guenser[1,2], Catherine Girard[3], Michele Mazza[4], Manuel Rigo[5] and Nicolas Goudemand[1]

[1]Ecole Normale Supérieure de Lyon, IGFL, CNRS UMR 5242, UCBL, 46 Allée d'Italie, F-69364 Lyon Cedex 07, France
[2]Univ. Lyon, Université Claude Bernard Lyon 1, LEHNA, CNRS UMR 5023, 3-6 rue Raphaël Dubois – Bâtiments Forel, 69622 Villeurbanne Cedex 43
[3]ISEM, Univ. Montpellier, CNRS, EPHE, IRD, Montpellier, France
[4]Largo Mazza, Piacenza, Italy
[5]Department of Geosciences, University of Padova, Via G. Gradenigo 6, 35131 Padova, Italy

CG, 0000-0003-3123-8276; NG, 0000-0002-2956-5852

Can we predict the evolutionary response of organisms to climate changes? The direction of greatest intraspecific phenotypic variance is thought to correspond to an *'evolutionary line of least resistance'*, i.e. a taxon's phenotype is expected to evolve along that general direction, if not constrained otherwise. In particular, heterochrony, whereby the timing or rate of developmental processes are modified, has often been invoked to describe evolutionary trajectories and it may be advantageous to organisms when rapid adaptation is critical. Yet, to date, little is known empirically as to which covariation patterns, whether static allometry, as measured in adult forms only, or ontogenetic allometry, the basis for heterochrony, may be prevalent in what circumstances. Here, we quantify the morphology of segminiplanate conodont elements during two distinct time intervals separated by more than 130 Myr: the Devonian-Carboniferous boundary and the Carnian-Norian boundary (Late Triassic). We evidence that the corresponding species share similar patterns of intraspecific static allometry. Yet, during both crises, conodont evolution was decoupled from this common evolutionary line of least resistance. Instead, it followed heterochrony-like trajectories that furthermore appear as driven by ocean temperature. This may have implications for our interpretation of conodonts' and past marine ecosystems' response to environmental perturbations.

## 1. Introduction

The ambition of evolutionary biology is to decipher the relative role of evolutionary processes in shaping the diversity of life. Because the evolution of new forms necessarily involves tinkering with the developmental processes of already existing forms [1], evolution is likely to follow trajectories that are biased by those developmental processes (see for instance [2] and references therein). In other words, some morphologies may be more readily generated than others (e.g. [3,4]) and this may drive evolution in preferential directions. For instance, the direction of greatest intraspecific phenotypic variance ($P_{max}$), as measured on adult forms only, is thought to correspond to an 'evolutionary line of least resistance', and morphological evolution is expected to parallel $P_{max}$ in a context of weak selection [5–8]. Similarly, heterochrony, whereby the timing or rate of developmental processes are modified within an individual or a taxon, can be considered as an alternative evolutionary line of least resistance and it has long been recognized as a key evolutionary pattern, with countless examples across the animal kingdom [2,9,10]. In the fossil record, this is exemplified by documented occurrences of paedomorphoclines (trend towards retention of juvenile characters in adults) or peramorphoclines (trend towards

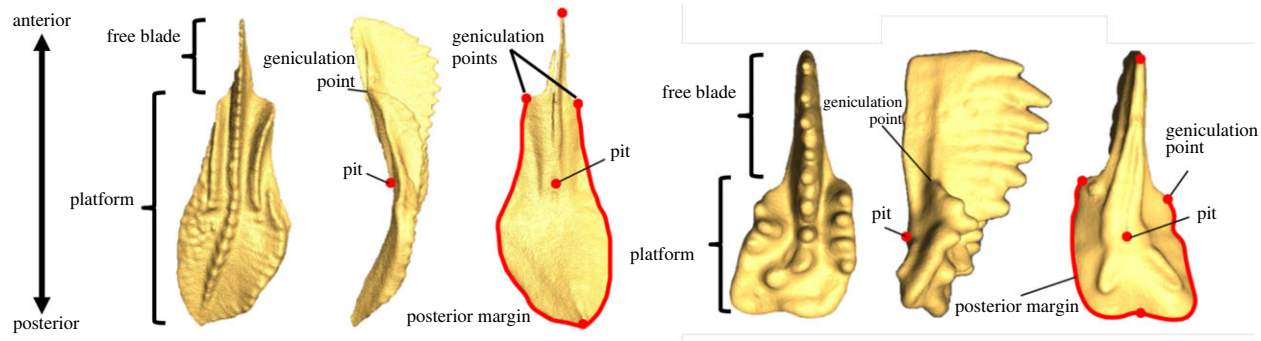


**Figure 1.** Anatomy of ozarkodinin segminiplanate elements and location of the traits of interest. Oral, lateral and aboral views of a $P_1$ element of *Siphonodella cooperi* (left, Carboniferous) and a $P_1$ element of *Epigondolella rigoi* (right, Late Triassic). The location of the used landmarks and sliding landmark curves are indicated in red. (Online version in colour.)

extension of growth period resulting in adding new developmental stages compared to ancestral sequence) [11–14]. Heterochronic shifts may produce large phenotypic effects with relatively few or no genetic modifications. They may then be particularly advantageous to organisms when rapid adaptation is critical, for instance during large environmental perturbations [11]. Yet, to date, little is known empirically as to which evolutionary mode, whether static allometry, as measured on adult forms only, and ontogenetic allometry, i.e. the patterns of covariation observed within an organism's growth, which are the support for heterochrony, may be prevalent in what circumstances.

Conodonts are extinct marine jawless vertebrates [15,16]. Their phosphatic feeding structures called conodont elements, are abundant in the fossil record from the Cambrian to the earliest Jurassic [17]. They are arranged in a complex feeding apparatus usually made of seven pairs and one central element. All of them display some level of morphological diversity. Yet the most dorsal pair of elements called $P_1$ exhibit a morphological diversity like no others, and some of the highest rates of morphological evolution of all Palaeozoic and Triassic fossils. Hence, they are used extensively for relative dating and correlating rocks (e.g. [18]). Some $P_1$ elements are considered to have had a mammal-like occlusion and they were probably used for crushing and processing food items [19]. Therefore, their morphology may reflect their feeding function and their bearer's diet. They are also useful for reconstructing the evolution of palaeoenvironments and environmental pressures (e.g. [20]). Yet, so far, the potential of the conodont fossil record for evolutionary studies has remained somewhat underexploited (but see for instance [21–24]). Several studies have implicitly highlighted patterns of covariation within conodont $P_1$ elements (e.g. [25]) and many conodont workers have observed morphological trends within specific intervals. Yet, no one to our knowledge has ever explored the universality of such patterns within conodonts. It is still unclear for instance whether the morphologies of conodont elements follow any generic rule of covariation. Similarly, the existence of commonalities between species in their evolutionary responses to distinct major events has never been tested.

Here, we quantified the morphological evolution of ozarkodinin (suborder Ozarkodinina Dzik 1976) segminiplanate $P_1$ elements around two distinct major intervals separated by about 130 Myr: siphonodellids (*Siphonodella*) from the Devonian-Carboniferous boundary (DC) and gondolellids (*Carnepigondolella*, *Epigondolella*, *Metapolygnathus*) from the Late Triassic Carnian-Norian boundary (CN). Both considered intervals are similarly long (respectively 5 Myr and 3 Myr) and were affected by putative global changes in sea-surface temperature: a 4° warming and a 6° cooling, respectively [26,27]. We focused on DC siphonodellids and CN gondolellids because the $P_1$ elements in both groups share superficial similarities that facilitate their comparison within a single empirical morphospace: they are segminiplanate [28], and possess both a variably ornamented platform and a relatively high blade that is partly free at the anterior end (figure 1). In both cases, the chosen material is abundant and well-preserved, and numerous previous studies have characterized or constrained their biochronology [18,29,30], ontogeny [31] and phylogeny [28,32–34] (figure 2).

Based on the suprageneric analysis of Donoghue *et al.* [35], these groups belong to two distinct superfamilies (siphonodellids and gondolellids) that probably diverged in the Ordovician, about 100 Myr before the first appearance of siphonodellids, which means both groups are separated by more than 300 Myr of independent evolution.

The present study quantifies morphological changes of these two assemblages through time. We evaluate the relative role of environmental and developmental processes as evolutionary forces driving their evolution and assess the impact of heterochronic shifts in observed evolutionary trends.

## 2. Results

### (a) Main morphological axes of variation

We used geometric morphometrics to quantify the intraspecific and interspecific patterns of variation of element shape within the two assemblages (see Methods). Only adult $P_1$ elements were considered ($GS_{4–6}$ in [31]). In conodont elements, identification of adulthood is based on empirical growth stages. For the considered taxa, the growth stages have been described by [36] and [31]. The position of the species in the morphospace is strongly correlated with its phylogenetic position (permutation test; two groups: $p$-value < 0.001; Carboniferous group only: $p$-value = 0.0093; Triassic group only: $p$-value = 0.0002). The holotypes of the species present in our collection are located within the respective 95% concentration ellipses (figure 3). Notwithstanding whether or not the holotype specimens were included in the dataset (see Methods), the principal component analysis (PCA) on the corresponding Procrustes coordinates showed that only four principal components (PCs) explained more than 5% of variance and are therefore considered significant (see methods and the electronic supplementary material,

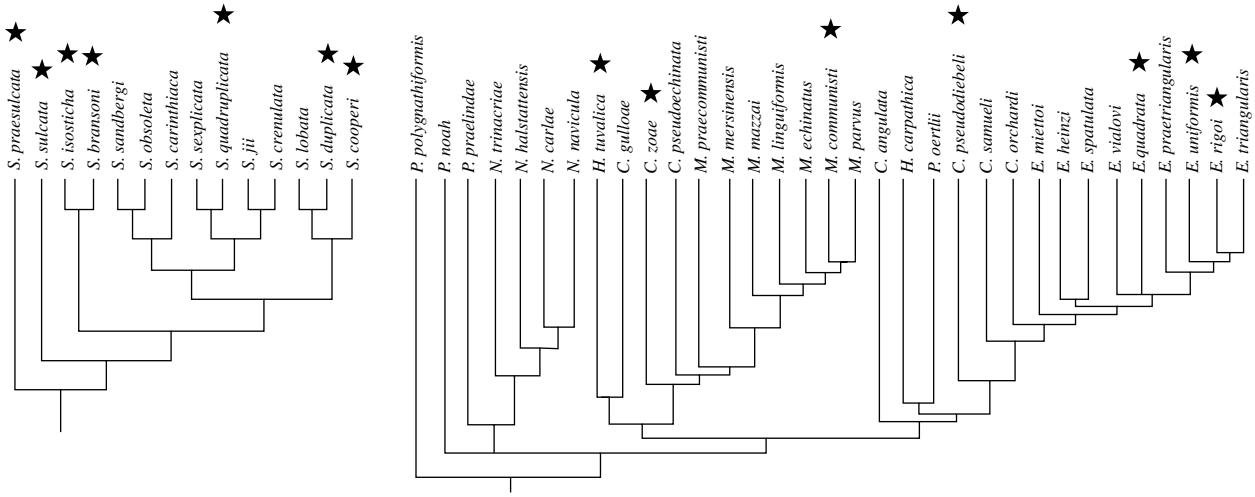


**Figure 2.** Phylogeny of the DC siphonodellids (left) and CN gondolellids (right). Modified respectively after [32] and [33]. *S.*, *Siphonodella*; *P.*, *Paragondolella*; *N.*, *Norigondolella*; *H.*, *Hayashiella*; *C.*, *Carnepigondolella*; *M.*, *Metapolygnathus*; *E.*, *Epigondolella*. Both *Hayashiella* and *Carnepigondolella* appear as polyphyletic. The stars designate species sampled in this study.

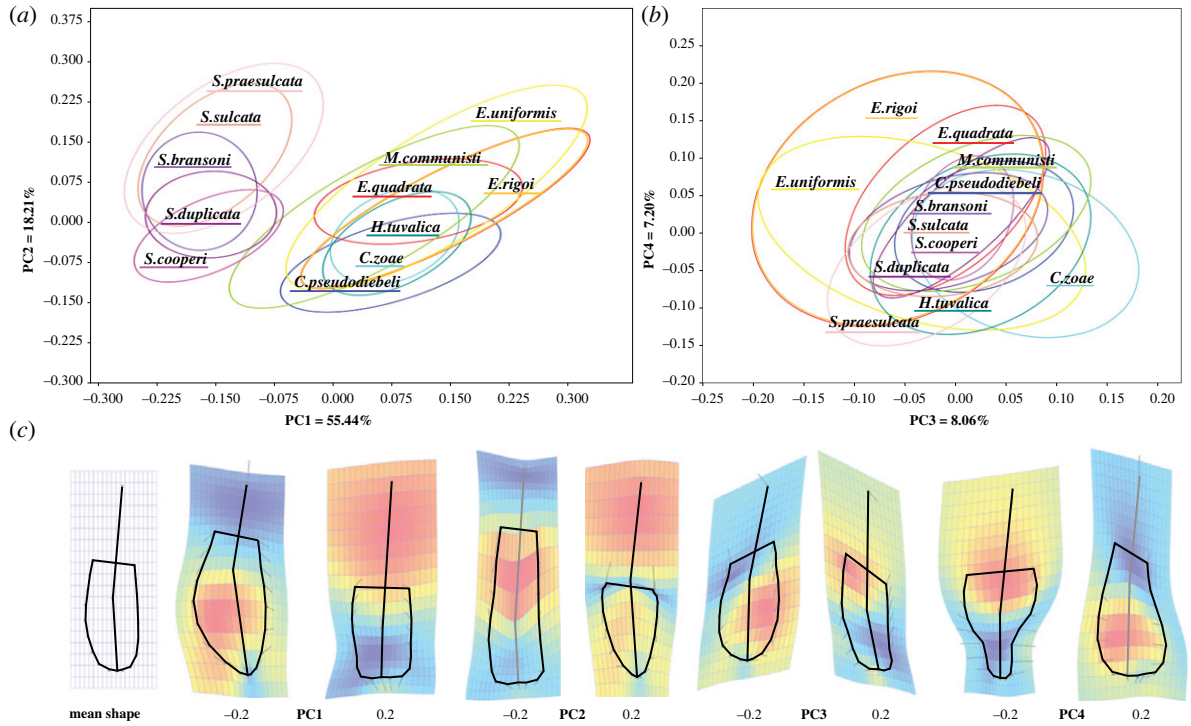


**Figure 3.** Principal component analysis of the morphologies of segminiplanate elements at the DC and CN boundaries. Scatterplots of the considered specimens on the PC1-PC2 plane (*a*), and PC3-PC4 plane (*b*) of the morphospace. Each species is coded by a distinct colour. The poorer data of *Siphonodella isosticha* and *Siphonodella quadruplicata* are not displayed here but available in the electronic supplementary material . The ellipses correspond to 95% of the variance of the corresponding species. In both planes, the ellipses appear aligned with one another, suggesting conservation of the patterns of intraspecific variation over large temporal and phylogenetic scales. (*c*) Thin-plate-splines deformation plots of each of the four significant principal components (PCs) relative to the consensus shape (left). Black lines connect landmarks to visualize reconstructed shape at given PC values. The hot-cold colour scale represents the expansion factors, the arrows represent the deformation vectors from consensus to given PC value (see [37]). (Online version in colour.)

figures S3–S4). When the holotypes are included, the first PCs explain about 83% (PC1: 49.93%, PC2: 18.19%, PC3: 7.82%, PC4: 7.01%) of the total variance of the Procrustes coordinates (see the electronic supplementary material, table S3). When they are not included, the first four PCs explain about 89% of the total variance (figure 3; electronic supplementary material, table S3; PC1: 55.44%, PC2: 18.21%, PC3: 8.06%, PC4: 7.20%). The main axis (PC1), which roughly discriminates between the DC taxa (siphonodellids, negative PC1 values) and the CN taxa (gondolellids, mostly positive PC1 values), corresponds to subequal, antero-posterior shifts of the pit and of the anterior ends of the platform (geniculation points), associated with a change in the curvature of the posterior platform margin: an anterior shift of the pit and geniculation points (negative PC1 values, DC taxa) corresponding to a more tapered posterior platform end (higher positive curvature), and a posterior shift (positive PC1 values, Triassic taxa) corresponding to a flatter (zero curvature) or even concave (negative curvature) posterior platform margin. In other words, DC taxa differ most from CN taxa by having $P_1$ elements whose platform is more extended anteriorly and pointier posteriorly and whose pit is located more anteriorly: DC taxa tend to have an ovate platform

with a pointed posterior extremity, whereas the CN taxa have an oblong to sub-cuneate platform with a rounded to sub-squared posterior margin.

Along PC2, the pit and geniculation points move in opposite directions along the antero-posterior axis (*contra* PC1; see the arrows in figure 3*c*). As along PC1, the antero-posterior shift of the pit is associated with a change in the curvature of the posterior platform margin. Extreme positive values of PC2 correspond to elements with a relatively short platform (and hence a relatively large free blade), a pit located in front of the geniculation points and a rounded to tapered posterior end, whereas extreme negative values of PC2 correspond to elements with a longer, narrower, anteriorly extended platform, a posterior pit and a flat to concave posterior end.

## (b) Covariation of the relative position of the pit and the shape of the posterior margin

As for PC1 and PC2, PC4 suggests a positive correlation between the relative distance of the pit to the posterior margin and the sharpening of the posterior margin, quantified as the curvature of the posterior margin at the posterior end (flat to circular to pointy geometry corresponding to a gradient from low to high curvature at the tip) (figure 3). In order to test for such correlation we ran a PCA analysis on a subset of our data where the Procrustes coordinates of the pit, anterior end and geniculation points were removed. The corresponding principal components ($PC_{contour}$) can be used as main descriptors of the changes in the platform outline, in particular of its posterior margin (electronic supplementary material, figure S9). We then verified (see Methods and the electronic supplementary material, figure S9) that the relative position of the pit within the element (the distance between the pit and the posterior margin divided by the element's length) is significantly correlated with the four main $PC_{contour}$ (electronic supplementary material, figure S9), in particular, it is strongly negatively correlated with $PC4_{contour}$ (Pearson' $r$ and Spearman's $D$-tests, $p < 10^{-20}$, $R^2 > 0.9$; see the electronic supplementary material, figure S9): the larger the distance, the narrower the posterior part of the platform relative to its anterior. In other words, when the pit is closer to the posterior margin, the posterior margin tends to be more squared; closer to the consensus, the posterior margin is sub-circular; when the pit is more anteriorly located, the posterior margin tends to taper to a point.

## (c) Long-term stability of $P_{max}$ within ozarkodinin conodonts

The $P_{max}$ of most species are aligned with one another ($\chi^2$ (same slope in PC1-PC2 plane) = 21.422; $p$-value = 0.0649; electronic supplementary material, figure S6). The relatively low number of measured specimens for *Siphonodella isoticha* and *Siphonodella quadruplicata* precludes an accurate linearization, leading to their $P_{max}$ not being aligned with that of other species. If these two species are removed, we obtain $\chi^2$ (same slope) = 13.898; $p$-value = 0.1259. The analysis of the within-group variation shows that most taxa share similar patterns of intraspecific variation among adults: they occupy roughly the same region of the PC1-$PC2_{within}$ morphospace and differ mostly along $PC3_{within}$ (Triassic taxa) or $PC4_{within}$ (DC taxa) (electronic supplementary material, figure S7). The main axis of this within-group variation ($PC1_{within}$) corresponds to an anterior extension (resp. reduction) of the platform associated with opposite movements of the geniculation points relative to the pit and anterior end (electronic supplementary material, figure S7). The second main axis ($PC2_{within}$) describes the amount of asymmetrical variation and corresponds approximately to the PC3 mentioned earlier.

The within group variation evolved mostly (and sub-monotonously) along the $PC4_{within}$ within siphonodellids (variation in the relative position of the pit and the shape of the posterior margin; see the electronic supplementary material, figure S7), whereas it evolved essentially along the $PC3_{within}$ among the CN taxa (variation in lateral expansion of the platform, see also [36]), that is, along axes that are, by construction, orthogonal to one another.

## (d) A common, main axis of morphological evolution that is distinct from $P_{max}$

Both groups vary essentially along the same axis within the PC1-PC2 plane of the empirical morphospace. We have reconstructed the likely chronological sequence of the considered taxa at both the generic and the species levels. For the siphonodellids the following sequence can be inferred from Sandberg's phylogenetic hypothesis ([32], his fig. 1), as supported by more recent works (e.g. [29]): *Siphonodella praesulcata* + *Siphonodella sulcata*, *Siphonodella bransoni* (=*Siphonodella duplicata* M1), *S. duplicata*, *Siphonodella cooperi*, *Siphonodella obsoleta* + *Siphonodella sandbergi* + *Siphonodella carinthiaca*, *S. quadruplicata*, *Siphonodella crenulata*. Notwithstanding whether we compute the average or the median of the PC2 scores of the taxa present in our collection or the PC2 scores of the holotypes, there is a significant decreasing trend in PC2 scores for the corresponding DC interval (Mann-Kendall test, $p < 0.05$; see the electronic supplementary material, file S12). Similarly, if we consider the sequence leading from *Carnepigondolella* (or '*Carnepigondolella*' 1 and 2, since *Carnepigondolella* appears as polyphyletic, see Material and Methods) to *Metapolygnathus* to *Epigondolella*, the average (and mean) PC scores of these genera increase monotonously. Using Tethyan range charts at the species level [18,38], we can derive a sequence of maximal association 'zones' (similar to Oppel zones; see the electronic supplementary material, file S12) and then compute the average (or mean) PC2 scores of the taxa present in a given 'zone' (using the scores of the holotypes). If we exclude the genus *Norigondolella*, whose range is discontinuous near the CN boundary [18], and consider only the carnepigondolellids, their descendants (*Metapolygnathus* and *Epigondolella*) and their probable ancestor *Paragondolella*, then there is a significant (submonotonous) increasing trend in PC2 scores (Mann-Kendall test, $S = -17$, $p = 0.0054$; see the electronic supplementary material, file S12).

Considering the current phylogenetic model, this increasing trend is paralleled in two distinct lineages: the one leading to *Metapolygnathus*, and the one leading to *Epigondolella*.

This pattern of morphological evolution highlights a common main evolutionary path sub-parallel to the PC2 axis. Yet, evolution proceeded in opposite directions at the Carnian-Norian boundary (increasing trend in PC2 scores) as compared to the DC boundary (decreasing trend in PC2 scores).

## (e) In both intervals the main evolutionary axis aligns with ontogenetic trajectories

Ontogenetic series are available for the present material. For the Triassic taxa in particular, those series have been reconstructed

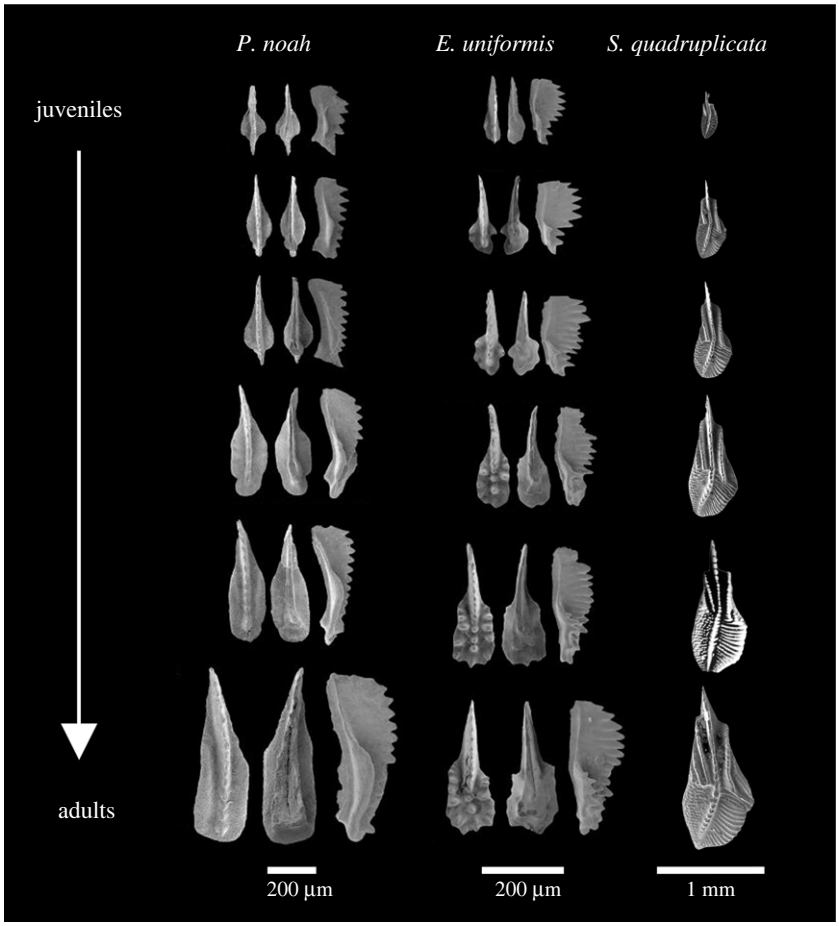


**Figure 4.** Growth series for *Paragondolella noah* (left), *Epigondolella uniformis* (centre) and *Siphonodella cooperi* (right). Modified after Mazza & Martinez-Perez [31] and Zhuravlev *et al*. [36].

in detail by Mazza & Martinez-Perez [31] using synchrotron-based imaging techniques and by virtually subtracting growth lamellae and analysing the evolution of the morphology within single adult specimens. The ontogeny in these species is marked by a relatively higher growth rate of the platform laterally and of both platform and blade towards the anterior side, which corresponds to a relative posterior shift of the pit (figure 4). For the siphonodellids, growth series have been proposed by Zhuravlev *et al*. [36] and display similar patterns (figure 4).

Within both groups (and more generally in most segminiplanate conodonts), the platform gets relatively larger with ontogenetic age, extending both anteriorly (the free blade gets relatively smaller in more mature individuals) and posteriorly: in species like *Paragondolella noah* and *Epigondolella uniformis* (figure 4), the posterior margin of the platform gradually changes from tapered to sub-circular to subquadrate. A similar transformation of the posterior margin is observed in all considered Late Triassic taxa. Similarly, in siphonodellids, the posterior margin of the platform is tapered throughout the ontogeny but it gets progressively broader and more rounded. Furthermore, in species like *E. uniformis* (figure 4), the pit may be initially located at the same level as the geniculation points along the antero-posterior axis. As the element grows and the platform extends anteriorly, this is no longer the case in ontogenetically older specimens. These descriptions, combined with the newly described correlation between the relative position of the pit and the shape of the platform's posterior margin, strongly suggest that morphologies associated with increasingly mature elements will get smaller (or more negative) scores on the PC2 axis.

Our results support previous observations by Zhuravlev *et al*. [36] and Mazza & Martinez-Perez [31]. The evolution of the considered DC taxa towards more anteriorly developed platforms with a posterior shift of the pit and a relative shortening of the free blade, is concordant with a peramorphosis heterochronic shift (a delayed maturation or faster development). Additionally, the evolution of the considered Triassic taxa towards elements with a less developed platform, an anteriorly shifted pit and an enlarged free blade, is compatible with a paedomorphosis shift (the retention of juvenile traits into adulthood). We argue that all considered taxa within one or the other group (DC taxa or CN taxa) share similar ontogenetic trajectories, namely a straight line along the PC2 axis. Similarly, we consider that most of their evolutionary trajectories follow the same line. In our view, the data is compatible with heterochrony being the main process involved, although not necessarily the only one.

## 3. Discussion

The putative peramorphocline of the DC siphonodellids and paedomorphocline of the CN gondolellids parallel respectively, and presumably time compatible, environmental shifts that are also opposite: the DC interval corresponds to a 4° warming of the oceans, whereas the CN interval corresponds to a 6° cooling. In other words, morphological change within both intervals parallels the PC2 axis, corresponds to a

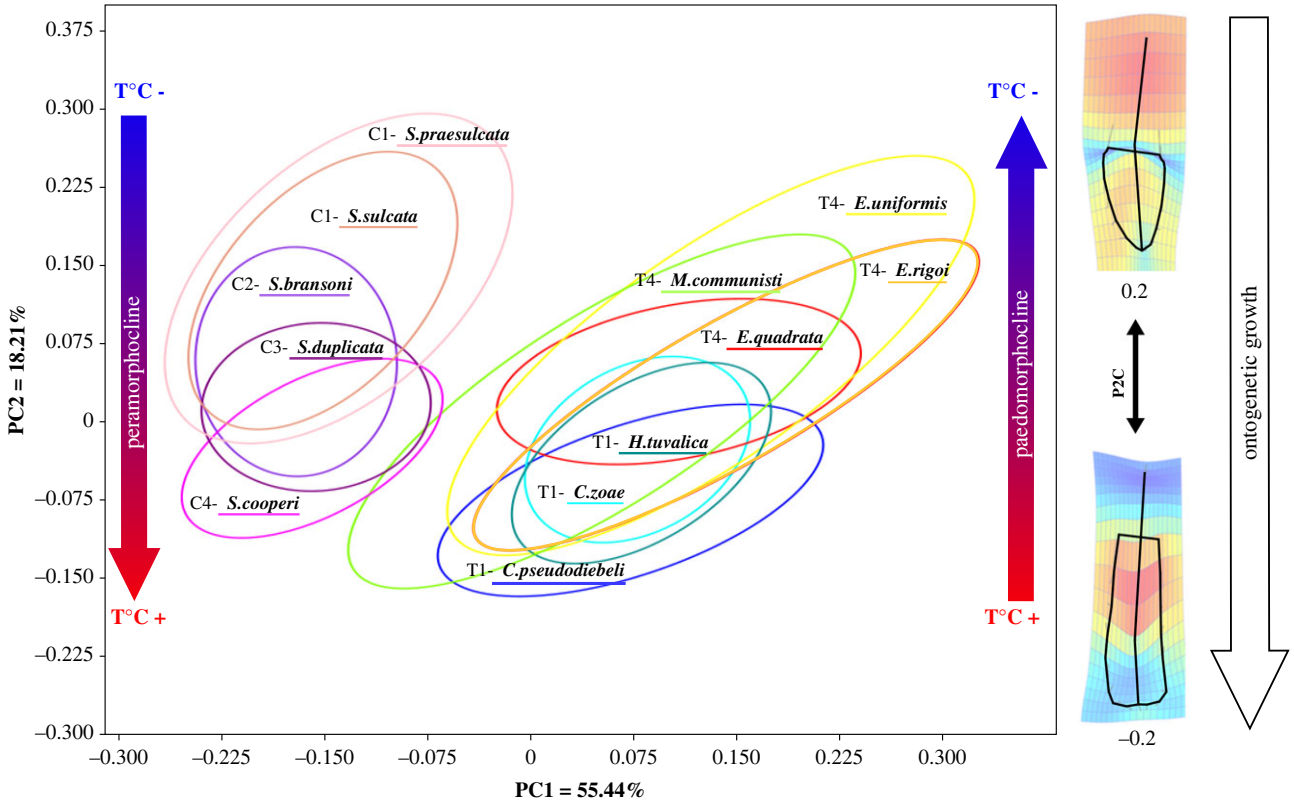


**Figure 5.** The direction of the heterochronic shifts at DC and CN boundaries may have been controlled by ocean temperature changes. Evolution at both boundaries parallels the PC2 axis (figure 3; electronic supplementary material). Ontogenetic growth also parallels the PC2 axis (figure 4), whereby low PC2 values correspond to developmentally older specimens and high PC2 values to younger specimens. The peramorphocline of DC siphonodellids corresponds to a global warming, the paedomorphocline of CN taxa to a global cooling, hence lower values of PC2 and mature forms correspond to higher temperatures. (Online version in colour.)

heterochronic shift, and is associated with a shift in seawater temperature, thereby suggesting that smaller PC2 values correspond to higher temperatures (figure 5).

Temperature is known to affect the growth rates of organisms [39–46]. For instance, aquatic ectotherms experience temperature-based phenotypic plasticity [47–50] and some of this plasticity may arise from altered growth rate. It is possible that temperature had a similar effect on the growth of conodont elements. Several authors have previously documented conodont morphoclines during intervals of environmental perturbations, in particular within Late Devonian genera (e.g. *Palmatolepis*, *Icriodus*, *Ancyrodella*, *Polygnathus*, but not *Siphonodella* until now) as responses to Late Devonian events such as the Kellwasser events (e.g. [25,51–53]). For instance, Renaud & Girard interpreted the evolutionary response of icriodids during these events as possibly involving paedomorphosis ('progenesis', [25, p. 31]). The respective responses of ancyrodellids, polygnathids or palmatolepids also parallel, to a certain extent, the palaeotemperature records ([54], but [53]), but they may or may not involve heterochronic shifts [25,51].

The latter authors tended to favour an indirect, ecological link over a physiological one: morphological modifications of dental elements are often related to functional shifts, i.e. associated with distinct feeding behaviours [55,56] and trophic disturbances have been indeed invoked for explaining the Kellwasser events [57]. Given that juvenile and adult conodonts do not necessarily share the same feeding habits [58], the two alternative propositions are not mutually exclusive and we can imagine scenarios whereby temperature-driven, physiologically induced heterochronic shifts may facilitate ecological adaptation to new, more abundant prey. Nonetheless, temperature is not the only factor that may impact conodonts' growth rate. Nutrient availability is a plausible alternative [54] that is also climate-dependent: a warmer climate usually implies more humidity, more weathering, more continental runoff, and may ultimately cause modifications in the communities of prey on which conodonts probably fed; it may also lead to eutrophication, and to hypoxia, another common agent of physiological changes. Ginot & Goudemand [59] have shown that conodonts may be affected by other abiotic factors, such as sea level (see also [53,60]), whose fluctuations may also parallel those of seawater temperatures. Hence, although temperature may appear as a plausible and attractively 'simple' driver (but see [61]) for the described evolutionary trajectories, its role is still elusive.

Because the groups considered here are distant in phylogeny, time, geography and probably ecology, the commonality of their evolutionary responses to climate changes may reflect some generic aspect of conodont's evolutionary biology. We propose here that some major aspect of the conodont element's development depended directly or indirectly on seawater temperature. Yet, as shown by Leu *et al.* [62], seawater temperature changes may have had contrasting effects on the evolution of different conodont taxa in terms of size. It is therefore expected that the pattern described here as a common response to temperature variation most likely accepts exceptions.

The long-term stability of the $P_{max}$ in these conodonts is somehow surprising. Static allometry (intraspecific variation among adults) is not expected to persist among related species [2,63], although evidence from the literature may be conflicting ([6], and references therein). This stability may be partly explained by the herein-described correlation between the relative position of the pit (respectively of the cusp) and the shape of the posterior margin. Similar

morphometric analyses have been performed on Late Devonian *Polygnathus* elements [53] and on Anisian (Middle Triassic) *Paragondolella* elements [64] and the corresponding plots seem to support the generality of such correlation. In both cases, the axis that reflects allometric growth ('PC2–3Dcar' in [53], their fig. 3; 'RW1' in [64], their fig. 6) corresponds also roughly to our PC2, thereby supporting our interpretation that this axis parallels ontogenetic and heterochronic shifts, and suggesting that it may be relevant to the evolutionary biology of many other conodont taxa.

Several authors have shown that the $G_{max}$, respectively the $P_{max}$, may be good, short-term predictors of evolutionary change (e.g. [7,65] and references therein). Long-term evolution however may be decoupled from within-population variation. Besides the fact that the nonlinear nature of the genotype-phenotype map of organs such as dental elements is expected to falsify the underlying linear models ([66], see also [67,68]) and may thus partly explain short-term discrepancies from those predictions, our results suggest that global environmental crises have the capacity to accelerate such decoupling (see also [69]). Here, the Late Devonian Hangenberg event and the late Carnian pluvial event may have forced conodonts to find evolutionary solutions to adapt to their changing environment. In both cases, conodonts seemingly resorted to heterochronic shifts that are compatible with some sort of temperature-induced 'evolutionary plasticity'.

# 4. Material and methods

## (a) Material and environmental context

The DC assemblage is composed of closely related species of *Siphonodella* from lower Tournaisian (Lower Mississipian, Carboniferous) rocks of Montagne Noire, France. The CN assemblage is composed of closely related species of *Carnepigondolella*, *Epigondolella*, *Metapolygnathus* and *Hayashiella* from upper Carnian and lower Norian (Upper Triassic) rocks of Pizzo Mondello, Sicily, Italy (figure 2).

The DC material was collected from the Puech de la Suque section in the Montagne Noire, France, and is currently housed in the collections of the Institut des Sciences de l'Evolution de Montpellier, France. It corresponds to a time-interval ranging from the *Siphonodella jii* Zone (PS17) to the *S. quadruplicata* Zone (PS28) and includes elements of eight species of the genus *Siphonodella*: *S. praesulcata*, *S. sulcata*, *S. bransoni*, *S. duplicata*, *S. carinthiaca*, *S. isosticha*, *S. quadruplicata* and *S. cooperi* (see the electronic supplementary material, table S1). To date, no cladistics-based phylogenetic hypotheses have been proposed for this clade. The most recurrent view [28,32] is that *S. praesulcata* were the rootstock of all siphonodellids (figure 2) of the late Devonian and early Mississipian (Carboniferous). The corresponding evolutionary radiation started first with the appearance of *S. sulcata* at (and possibly marking) the Devonian/Carboniferous boundary, followed by those of *S. bransoni (duplicata* morphotype 1) and *S. duplicata*. The latter two species are considered as the ancestors of all the younger siphonodellids, which emerged during the upper *duplicata* Zone (now *jii* Zone). The material originates from an interval that begins approximately 0.5 Myr after the Devonian/Carboniferous boundary and extends over 2 Myr. Locally at the Puech de la Suque section, this period is marked by a regression-transgression cycle, with sediments corresponding to a shallow dip into the photic zone, followed by a slow deepening beyond the photic zone [70]. Globally, the stable oxygen isotope ratios ($\delta^{18}O$) measured on conodont apatite from Europe and Laurentia evidence a mean global negative shift of about 1‰ from the top of the Hangenberg event to the *quadruplicata* Zone, which corresponds to an average global 4° warming of the ocean waters [26]. This global warming is associated with a coeval 1.5‰ drop of the stable carbon isotope ratio ($\delta^{13}C$) as measured on carbonates [26].

The Triassic material, housed in the collections of the Dipartimento di Scienze della Terra ' A. Desio ' (Università degli Studi di Milano) and at the Department of Geosciences (University of Padova), is from the Pizzo Mondello section, located in the Sicani Mountains, Western Sicily, Italy. The elements belong to seven species, currently arranged in four genera: *Carnepigondolella pseudodiebeli*, and *Carnepigondolella zoae*; *Hayashiella tuvalica*; *Epigondolella quadrata*, *Epigondolella rigoi* and *E. uniformis*; and *Metapolygnathus communisti* (electronic supplementary material, table S1). We follow here the cladistics-based phylogenetic model proposed by Mazza *et al*. [33]. *Paragondolella polygnathiformis and Paragondolella praelindae* were presumably the only two species to survive the Carnian Pluvial event. They gave rise to the genera *Carnepigondolella* and *Norigondolella*. *Carnepigondolella* itself appears to be a polyphyletic group that would have branched into, on one hand *Metapolygnathus* and, on the other hand, *Epigondolella*. Recently, Kilic *et al*. [71] reassigned '*Carnepigondolella' tuvalica* and '*Carnepigondolella' carpathica* to a new genus *Hayashiella*, from which, in their view, all carnepigondolellids stemmed. Yet, this is not supported by the analysis of Mazza *et al*. [33] as *Hayashiella* would appear polyphyletic too. Alternatively, it might be convenient (although not optimal) to group the carnepigondolellids (including *Hayashiella*) leading to *Metapolygnathus* on one hand and the ones leading to *Epigondolella* on the other, as two distinct paraphyletic groups (coined here '*Carnepigondolella*' 1 and '*Carnepigondolella*' 2). Based on abundant material from Black Bear Ridge, British Columbia, Canada, Orchard proposed a different taxonomical approach to Carnian-Norian 'platform' conodonts [72,73], which initially rendered comparisons with conodonts from Pizzo Mondello very challenging. In a more recent work, Orchard [34] suggested that many taxa previously considered as endemic to Black Bear Ridge or to Pizzo Mondello were in fact shared by the two localities and he proposed numerous synonymies. Because the generic classification of Orchard emphasizes somewhat arbitrarily (but possibly rightfully so) the configuration of the anterior platform margins over platform shape, posterior ornament, relative blade-carina length, and pit position, we have preferred here the arguably more agnostic cladistic approach adopted by Mazza *et al*. [33]. It is noteworthy that despite the differences in taxonomic approaches, the same evolutionary trends are common at both localities ([34], p. 54). The studied interval, ranging from the *P. polygnathiformis* Zone to the *E. rigoi-E.quadrata* Zone, spans the Carnian-Norian boundary (CNB, Late Triassic). This interval corresponds to a major conodont turnover subsequent to the Carnian Pluvial Event [74,75]. The rocks of the Pizzo Mondello section record a less than 1‰ positive shift of the $\delta^{13}C$ at the base of the CNB interval [74,76]. Although there is no local evidence for any change in seawater temperatures or in sea level (see also [77]), a positive shift of 1.5‰ has been reported by Trotter *et al*. [27] in the $\delta^{18}O$ signal at the wider scale of the sub-tropical Tethys, evidencing a presumed global 6°C cooling of the oceans (see also [78]).

All studied elements are considered adult forms following the growth stages as defined and illustrated by [36] and [31], respectively. Since most authors adopt a typological approach, and although the morphological variation within a given species is likely to evolve in time, we assume here that any significant evolutionary change within a species would have led authors to define a new species. In other words, we assume that the herein estimated intraspecific variation (and hence the $P_{max}$) of the considered species approximate accurately the 'true' intraspecific variation of those taxa, despite being based on one location and for some species on one horizon only (electronic supplementary material, table S1). This is a relatively strong hypothesis but it is in our view justified by the large temporal and taxonomic breadth of our study.

In order to assess the validity of the observed evolutionary patterns across the corresponding evolutionary lineages, we considered additionally the holotypes of all the species belonging to the considered genera, as based on the considered phylogenies (figure 2), irrespective of whether they were present or not in our collections. In those rare cases where the illustrations of the holotypes available from the literature were not appropriate for our analysis (e.g. broken specimens), we selected alternative, well-preserved, complete specimens from the literature (see details in the electronic supplementary material, table S2).

## (b) Digitization

All the elements were glued on wooden sticks and digitized at 1 µm cubic voxel resolution using a Phoenix nanotomeS X-ray microtomograph ($\mu$CT, AniRA-Immos platform, SFR Biosciences, UMS 3444, ENS Lyon). The element surfaces were reconstructed in three-dimensional and pictures were taken in a standardized aboral view (figure 1) using the Amira software (v. 6.3.0). For comparison purposes, dextral elements were mirrored into virtual sinistral ones and lumped together. No systematic differences between sinistral and dextral elements were found after this transformation according to a multivariate analysis of variance (PERMANOVA, $p$-value < 0.0001).

## (c) Geometric morphometrics

Throughout the life of a conodont, the feeding elements were not shed and replaced as in polyphyodont vertebrates but retained and grown/repaired via outer-apposition of new growth lamellae [79,58]. This mode of growth, which resembles that of ganoid scales in fishes, implies for instance gradual addition—and sometimes fusion—of denticles, and renders the definition of biologically homologous parts and hence the quantitative comparison of conodonts elements particularly challenging [80,81]. To quantify the shape of the elements, we adopted a landmark-based approach using TPSDig 2.0 [82]: five landmarks were digitized that correspond to the anterior and posterior extremities of the elements, the growth centre of the element (the so-called pit), and the antero-lateral extremities of the platform (the so-called geniculation points). Two sets of 10 equally distributed sliding landmarks were also digitized on the platform margins between the geniculation points and the posterior extremity (figure 1; electronic supplementary material, figure S10). Ornamentation features may be critical for distinguishing between two closely related species but it is challenging to quantify those in a way that would be relevant for comparison between Carboniferous and Triassic forms. Hence, ornamentation was not taken into account in the present study.

All measured individuals were subjected to a generalized full Procrustes superimposition using the two sets of landmarks in TPSRelw [83]. This procedure allows us to standardize the configurations of landmarks for scale and orientation. The Procrustes coordinates (individual residuals to the resulting consensus) were used as shape variables in the subsequent analyses. Deformations along the axes of the PCA were visualised using the 'Geometry/Landmarks/PCA' function in PAST ([37], v. 4.05).

## (d) Statistics

The Procrustes coordinates were analysed using a PCA on the variance-covariance matrix using the above-mentioned function in PAST [37]. Only the axes explaining more than 5% of variance were considered significant and included in subsequent analysis (see the electronic supplementary material, figures S3–S4). An option in that software allows us to assess within-group variation, where the average within each group is subtracted prior to eigenanalysis, essentially removing the differences between groups. For the general case ('Disregard groups' option), 1000 iterations were computed using the bootstrap option. Shape differences between genera were tested using a PERMANOVA (non-parametric multivariate analysis of variance based on 9999 permutations) and associated pairwise *post-hoc* tests. Following protocol from [38], $P_{max}$ is estimated as the reduced major axes (RMA) of each species and was calculated on PC1 and PC2 of the total dataset without holotypes. This regression is specifically formulated to handle errors in both the $x$ and $y$ variables by minimizing the sum of the areas (thus using both vertical and horizontal distances of the data points from the resulting line) [84]. Slopes differences were tested using the $\chi^2$ test for multiple comparison of RMA slopes available in PAST. The significance of the phylogenetic structure of the morphospace has been tested using a permutation test against the null hypothesis of no phylogenetic signal (1000 iterations) using the MorphoJ software [85]. Temporal trends were tested using the non-parametric Mann-Kendall test (as implemented in the 'Timeseries' module of PAST, [37]) and correlations were assessed using Pearson (linear $r$) and Spearman's D statistics (as implemented in the 'Univariate' module of PAST, [37]). The trend is documented against ranked temporal position for the CN fauna at the generic level and for the DC siphonodellids at the species level (under two slightly different ways of classifying DC taxa). In both cases those sequences are consensual at those levels.

Data accessibility. The morphometry are available at the following links, (DC specimens: http://morphobank.org/permalink/?P4424; CN specimens: http://morphobank.org/permalink/?P4048). The morphometrical data is available in the electronic supplementary material [86].

Authors' contributions. L.S.: data curation, formal analysis, investigation, methodology, writing—original draft, writing—review and editing; P.G.: data curation, formal analysis, investigation, methodology, writing—review and editing; C.G.: resources, writing—review and editing; M.M.: resources, writing—review and editing; M.R.: resources, writing—review and editing; N.G.: conceptualization, formal analysis, funding acquisition, investigation, methodology, project administration, supervision, validation, writing—original draft, writing—review and editing.

All authors gave final approval for publication and agreed to be held accountable for the work performed therein.

Conflict of interest declaration. We declare we have no competing interests.

Funding. This research was supported by a French ANR @ RAction grant to NG (project 'EvoDevOdonto').

Acknowledgements. We warmly thank Mathilde Bouchet for her assistance with the AniRA-ImOss platform of microtomography (SFR Biosciences, ENS Lyon), and Carlo Corradini for his help with the taxonomy of siphonodellids.

# References

1. Jacob F. 1977 Evolution and tinkering. *Science* **196**, 1161–1166. (doi:10.1126/science.860134)
2. Jablonski D. 2020 Developmental bias, macroevolution, and the fossil record. *Evol. Dev.* **22**, 103–125. (doi:10.1111/ede.12313)
3. Beldade P, Koops K, Brakefield PM. 2002 Developmental constraints versus flexibility in morphological evolution. *Nature* **416**, 844–847. (doi:10.1038/416844a)
4. Kavanagh KD, Shoval O, Winslow BB, Alon U, Leary BP, Kan A, Tabin CJ. 2013 Developmental bias in the evolution of phalanges. *Proc. Natl Acad. Sci. USA* **110**, 18 190–18 195. (doi:10.1073/pnas.1315213110)
5. Schluter D. 1996 Adaptive radiation along genetic lines of least resistance. *Evolution* **50**, 1766–1774. (doi:10.1111/j.1558-5646.1996.tb03563.x)

6. Renaud S, Auffray J-C, Michaux J. 2006 Conserved phenotypic variation patterns, evolution along lines of least resistance, and departure due to selection in fossil rodents. *Evolution* **60**, 1701–1717. (doi:10.1111/j.0014-3820.2006.tb00514.x)
7. Haber A. 2016 Phenotypic covariation and morphological diversification in the ruminant skull. *Am. Nat.* **187**, 576–591. (doi:10.1086/685811)
8. Hunt G. 2007 Evolutionary divergence in directions of high phenotypic variance in the ostracode genus *Poseidonamicus*. *Evolution* **61**, 1560–1576. (doi:10.1111/j.1558-5646.2007.00129.x)
9. Morris ZS, Vliet KA, Abzhanov A, Pierce SE. 2019 Heterochronic shifts and conserved embryonic shape underlie crocodylian craniofacial disparity and convergence. *Proc. R. Soc. B* **286**, 20182389. (doi:10.1098/rspb.2018.2389)
10. Urdy S, Wilson LA, Haug JT, Sánchez-Villagra MR. 2013 On the unique perspective of paleontology in the study of developmental evolution and biases. *Biol. Theory* **8**, 293–311. (doi:10.1007/s13752-013-0115-1)
11. McNamara KJ. 2012 Heterochrony: the evolution of development. *Evol.: Educ. Outreach* **5**, 203–218. (doi:10.1007/s12052-012-0420-3)
12. Solovjev AN. 2015 Heterochrony and heterotopy in the phylogeny of sea urchins. *Paleontol. J.* **49**, 1582–1596. (doi:10.1134/S0031030115140191)
13. Gerber S. 2011 Comparing the differential filling of morphospace and allometric space through time: the morphological and developmental dynamics of Early Jurassic ammonoids. *Paleobiology* **37**, 369–382. (doi:10.1666/10005.1)
14. Monnet C, Klug C, De Baets K. 2015 Evolutionary patterns of ammonoids: phenotypic trends, convergence, and parallel evolution. In *Ammonoid paleobiology* (eds C Klug, D Korn, K De Baets, I Kruta, RH Mapes), pp. 95–142. Amsterdam, The Netherlands: Springer.
15. Aldridge RJ, Briggs DEG, Smith MP, Clarkson ENK, Clark NDL. 1993 The anatomy of conodonts. *Phil. Trans. R. Soc. Lond. B* **340**, 405–421. (doi:10.1098/rstb.1993.0082)
16. Donoghue PC, Forey PL, Aldridge RJ. 2000 Conodont affinity and chordate phylogeny. *Biol. Rev.* **75**, 191–251. (doi:10.1017/S0006323199005472)
17. Du Y, Chiari M, Karádi V, Nicora A, Onoue T, Pálfy J, Roghi G, Tomimatsu Y, Rigo M. 2020 The asynchronous disappearance of conodonts: new constraints from Triassic-Jurassic boundary sections in the Tethys and Panthalassa. *Earth Sci. Rev.* **203**, 103176. (doi:10.1016/j.earscirev.2020.103176)
18. Rigo M, Mazza M, Karádi V, Nicora A. 2018 New Upper Triassic conodont biozonation of the Tethyan realm. In *The Late Triassic world* (ed. LH Tanner), pp. 189–235, Berlin, Germany: Springer.
19. Donoghue PC, Purnell MA. 1999 Mammal-like occlusion in conodonts. *Paleobiology* **25**, 58–74.
20. Romano C, Goudemand N, Vennemann T, Ware D, Schneebeli-Hermann E, Hochuli PA, Brühwiler T, Brinkmann W, Bucher H. 2013 Climatic and biotic upheavals following the end-Permian mass extinction. *Nat. Geosci.* **6**, 57–60. (doi:10.1038/ngeo1667)
21. Roopnarine PD. 2005 The likelihood of stratophenetic-based hypotheses of genealogical succession. *Spec. Pap. Palaeontol.* **73**, 143–157.
22. Barnett SG. 1972 The evolution of *Spathognathodus remscheidensis* in New York, New Jersey, Nevada, and Czechoslovakia. *J. Paleontol.* **46**, 900–917.
23. Girard C, Renaud S, Korn D. 2004 Step-wise morphological trends in fluctuating environments: evidence in the Late Devonian conodont genus *Palmatolepis*. *Geobios* **37**, 404–415. (doi:10.1016/j.geobios.2003.07.002)
24. Jones D. 2009 Directional evolution in the conodont *Pterospathodus*. *Paleobiology* **35**, 413–431. (doi:10.1666/0094-8373-35.3.413)
25. Renaud S, Girard C. 1999 Strategies of survival during extreme environmental perturbations: evolution of conodonts in response to the Kellwasser crisis (Upper Devonian). *Palaeogeogr. Palaeoclimatol. Palaeoecol.* **146**, 19–32. (doi:10.1016/S0031-0182(98)00138-2)
26. Buggisch W, Joachimski MM, Sevastopulo G, Morrow JR. 2008 Mississippian $\delta$13Ccarb and conodont apatite $\delta$18O records—their relation to the Late Palaeozoic Glaciation. *Palaeogeogr. Palaeoclimatol. Palaeoecol.* **268**, 273–292. (doi:10.1016/j.palaeo.2008.03.043)
27. Trotter JA, Williams IS, Nicora A, Mazza M, Rigo M. 2015 Long-term cycles of Triassic climate change: a new $\delta$18O record from conodont apatite. *Earth Planet. Sci. Lett.* **415**, 165–174. (doi:10.1016/j.epsl.2015.01.038)
28. Sweet WC. 1988 *The conodonta: morphology, taxonomy, paleoecology, and evolutionary history of a long-extinct animal phylum*. Oxford, UK: Clarendon Press.
29. Corradini C, Spaletta C, Mossoni A, Matyja H, Over D. 2017 Conodonts across the Devonian/Carboniferous boundary: a review and implication for the redefinition of the boundary and a proposal for an updated conodont zonation. *Geol. Mag.* **154**, 888–902. (doi:10.1017/S0016756816000039X)
30. Mazza M, Rigo M, Gullo M. 2012 Taxonomy and biostratigraphic record of the Upper Triassic conodonts of the Pizzo Mondello section (western Sicily, Italy), GSSP candidate for the base of the Norian. *Riv. Ital. Paleontol. Stratigr.* **118**, 85–130.
31. Mazza M, Martinez-Perez C. 2015 Unravelling conodont (Conodonta) ontogenetic processes in the Late Triassic through growth series reconstructions and X-ray microtomography. *Boll. Soc. Paleontol. Ital.* **54**, 161–186.
32. Sandberg CA, Ziegler W, Leuteritz K, Brill SM. 1978 Phylogeny, speciation, and zonation of *Siphonodella* (Conodonta, upper Devonian and lower Carboniferous). *Newsl. Stratigr.* **7**, 102–120. (doi:10.1127/nos/7/1978/102)
33. Mazza M, Cau A, Rigo M. 2012 Application of numerical cladistic analyses to the Carnian–Norian conodonts: a new approach for phylogenetic interpretations. *J. Syst. Paleontol.* **10**, 401–422. (doi:10.1080/14772019.2011.573584)
34. Orchard MJ. 2019 The Carnian-Norian GSSP candidate at Black Bear Ridge, British Columbia, Canada: update, correlation and conodont taxonomy. *Albertiana* **45**, 50–68.
35. Donoghue PCJ, Purnell MA, Aldridge RJ, Zhang SX. 2008 The interrelationships of 'complex' conodonts (Vertebrata). *J. Syst. Paleontol.* **6**, 119–153. (doi:10.1017/S1477201907002234)
36. Zhuravlev AV, Plotitsyn AN, Cígler V, Kumpan T. 2021 Taxonomic notes on some advanced Tournaisian (Mississippian) siphonodellids (Conodonta). *Geobios* **64**, 93–101. (doi:10.1016/j.geobios.2020.12.001)
37. Hammer Ø, Harper DAT, Ryan PD. 2001 PAST: paleontological statistics software package for education and data analysis. *Palaeontol. Electron.* **4**, 9.
38. Guenser P, Souquet L, Dolédec S, Mazza M, Rigo M, Goudemand N. 2019 Deciphering the roles of environment and development in the evolution of a Late Triassic assemblage of conodont elements. *Paleobiology* **45**, 440–457. (doi:10.1017/pab.2019.14)
39. Bachmann K. 1969 Temperature adaptations of amphibian embryos. *Am. Nat.* **103**, 115–130. (doi:10.1086/282588)
40. Blaxter JHS. 1969 Development: eggs and larvae. In *Fish physiology*, vol. 3 (eds WS Hoar, DJ Randall), pp. 177–252. Cambridge, MA: Academic Press.
41. Brown HA. 1967 Embryonic temperature adaptations and genetic compatibility in two allopatric populations of the spadefoot toad, *Scaphiopus hammondi*. *Evolution* **21**, 742–761. (doi:10.1111/j.1558-5646.1967.tb03431.x)
42. Brown HA. 1975 Temperature and development of the tailed frog, *Ascaphus truei*. *Comp. Biochem. Physiol. Part A: Physiol.* **50**, 397–405. (doi:10.1016/0300-9629(75)90033-X)
43. Brown HA. 1976 The time–temperature relation of embryonic development in the northwestern salamander, *Ambystoma gracile*. *Can. J. Zool.* **54**, 552–558. (doi:10.1139/z76-063)
44. Kuramoto M. 1975 Embryonic temperature adaptation in development rate of frogs. *Physiol. Zool.* **48**, 360–366. (doi:10.1086/physzool.48.4.30155661)
45. McLaren IA. 1965 Some relationships between temperature and egg size, body size, development rate, and fecundity, of the copepod *Pseudocalanus*. *Limnol. Oceanogr.* **10**, 528–538. (doi:10.4319/lo.1965.10.4.0528)
46. Huss M, Lindmark M, Jacobson P, van Dorst RM, Gårdmark A. 2019 Experimental evidence of gradual size-dependent shifts in body size and growth of fish in response to warming. *Glob. Change Biol.* **25**, 2285–2295. (doi:10.1111/gcb.14637)
47. Bizuayehu TT, Johansen SD, Puvanendran V, Toften H, Babiak I. 2015 Temperature during early development has long-term effects on microRNA expression in Atlantic cod. *BMC Genom.* **16**, 305. (doi:10.1186/s12864-015-1503-7)
48. Hollowed AB *et al.* 2013 Projected impacts of climate change on marine fish and fisheries. *ICES J. Mar. Sci.* **70**, 1023–1037. (doi:10.1093/icesjms/fst081)

49. Petitgas P, Rijnsdorp AD, Dickey-Collas M, Engelhard GH, Peck MA, Pinnegar JK, Drinkwater K, Huret M, Nash RD. 2013 Impacts of climate change on the complex life cycles of fish. *Fish. Oceanogr.* **22**, 121–139. (doi:10.1111/fog.12010)
50. Rowiński PK, Mateos-Gonzalez F, Sandblom E, Jutfelt F, Ekström A, Sundström LF. 2015 Warming alters the body shape of European perch *Perca fluviatilis*. *J. Fish Biol.* **87**, 1234–1247. (doi:10.1111/jfb.12785)
51. Girard C, Renaud S, Feist R. 2007 Morphometrics of the Late Devonian conodont genus *Palmatolepis*: phylogenetic, geographical and ecological contributions of a generic approach. *J. Micropalaeontol.* **26**, 61–72. (doi:10.1144/jm.26.1.61)
52. Girard C, Renaud S. 2008 Disentangling allometry and response to Kellwasser anoxic events in the Late Devonian conodont genus *Ancyrodella*. *Lethaia* **41**, 383–394. (doi:10.1111/j.1502-3931.2008.00095.x)
53. Renaud S, Ecalle B, Claisse P, Charruault A, Ledevin R, Girard C. 2020 Patterns of bilateral asymmetry and allometry in Late Devonian *Polygnathus* conodonts. *Palaeontology* **64**, 137–159. (doi:10.1111/pala.12513)
54. Balter V, Renaud S, Girard C, Joachimski MM. 2008 Record of climate-driven morphological changes in 376 Ma Devonian fossils. *Geology* **36**, 907–910. (doi:10.1130/G24989A.1)
55. Streelman JT, Webb JF, Albertson RC, Kocher TD. 2003 The cusp of evolution and development: a model of cichlid tooth shape diversity. *Evol. Dev.* **5**, 600–608. (doi:10.1046/j.1525-142X.2003.03065.x)
56. Ward-Campbell BMS, Beamish FWH, Kongchaiya C. 2005 Morphological characteristics in relation to diet in five coexisting Thai fish species. *J. Fish Biol.* **67**, 1266–1279. (doi:10.1111/j.1095-8649.2005.00821.x)
57. Racki G, Racka M, Matyja H, Devleeschouwer X. 2002 The Frasnian–Famennian boundary interval in the South Polish–Moravian shelf basins: integrated event-stratigraphical approach. *Palaeogeogr. Palaeoclimatol. Palaeoecol.* **181**, 251–297. (doi:10.1016/S0031-0182(01)00481-3)
58. Shirley B, Grohganz M, Bestmann M, Jarochowska E. 2018 Wear, tear and systematic repair: testing models of growth dynamics in conodonts with high-resolution imaging. *Proc. R. Soc. B* **285**, 20181614. (doi:10.1098/rspb.2018.1614)
59. Ginot S, Goudemand N. 2020 Global climate changes account for the main trends of conodont diversity but not for their final demise. *Glob. Planetary Change* **195**, 103325. (doi:10.1016/j.gloplacha.2020.103325)
60. Petryshen W, Henderson CM, De Baets K, Jarochowska E. 2020 Evidence of parallel evolution in the dental elements of *Sweetognathus* conodonts. *Proc. R. Soc. B* **287**, 20201922. (doi:10.1098/rspb.2020.1922)
61. Spicer JI, Burggren WW. 2003 Development of physiological regulatory systems: altering the timing of crucial events. *Zoology* **106**, 91–99. (doi:10.1078/0944-2006-00103)
62. Leu M, Bucher H, Goudemand N. 2019 Clade-dependent size response of conodonts to environmental changes during the late Smithian extinction. *Earth Sci. Rev.* **195**, 52–67. (doi:10.1016/j.earscirev.2018.11.003)
63. Voje KL, Hansen TF, Egset CK, Bolstad GH, Pélabon C. 2014 Allometric constraints and the evolution of allometry. *Evolution* **68**, 866–885. (doi:10.1111/evo.12312)
64. Chen Y, Neubauer TA, Krystyn L, Richoz S. 2016 Allometry in Anisian (Middle Triassic) segminiplanate conodonts and its implications for conodont taxonomy. *Palaeontology* **59**, 725–741. (doi:10.1111/pala.12253)
65. Hansen TF, Houle D. 2008 Measuring and comparing evolvability and constraint in multivariate characters. *J. Evol. Biol.* **21**, 1201–1219. (doi:10.1111/j.1420-9101.2008.01573.x)
66. Milocco L, Salazar-Ciudad I. 2020 Is evolution predictable? Quantitative genetics under complex genotype-phenotype maps. *Evolution* **74**, 230–244. (doi:10.1111/evo.13907)
67. Alberch P. 1980 Ontogenesis and morphological diversification. *Am. Zool.* **20**, 653–667. (doi:10.1093/icb/20.4.653)
68. Polly PD. 2008 Developmental dynamics and G-matrices: can morphometric spaces be used to model phenotypic evolution? *Evol. Biol.* **35**, 83–96. (doi:10.1007/s11692-008-9020-0)
69. Brombacher A, Wilson PA, Bailey I, Ezard THG. 2017 The breakdown of static and evolutionary allometries during climatic upheaval. *Am. Nat.* **190**, 350–362. (doi:10.1086/692570)
70. Girard C. 1994 Conodont biofacies and event stratigraphy across the D/C boundary in the stratotype area (Montagne Noire, France). *Cour. Forschungsinstitut Senckenberg* **168**, 299–309.
71. Kiliç AM, Plasencia P, Ishida K, Hirsch F. 2015 The case of the Carnian (Triassic) conodont genus *Metapolygnathus* Hayashi. *J. Earth Sci.* **26**, 219–223. (doi:10.1007/s12583-015-0534-y)
72. Orchard M. 2013 Five new genera of conodonts from the Carnian-Norian Boundary beds, northeast British Columbia, Canada. *New Mexico Mus. Nat. Hist. Sci. Bull.* **61**, 445–457.
73. Orchard M. 2014 Conodonts from the Carnian-Norian Boundary (Upper Triassic) of Black Bear Ridge, northeastern British Columbia, Canada. *New Mexico Mus. Nat. Hist. Sci. Bull.* **64**, 1–139.
74. Mazza M, Furin S, Spötl C, Rigo M. 2010 Generic turnovers of Carnian/Norian conodonts: climatic control or competition? *Palaeogeogr. Palaeoclimatol. Palaeoecol.* **290**, 120–137. (doi:10.1016/j.palaeo.2009.07.006)
75. Rigo M, Preto N, Roghi G, Tateo F, Mietto P. 2007 A rise in the carbonate compensation depth of western Tethys in the Carnian (Late Triassic): deep-water evidence for the Carnian Pluvial Event. *Palaeogeogr. Palaeoclimatol. Palaeoecol.* **246**, 188–205. (doi:10.1016/j.palaeo.2006.09.013)
76. Muttoni G, Kent DV, Olsen PE, Stefano PD, Lowrie W, Bernasconi SM, Hernández FM. 2004 Tethyan magnetostratigraphy from Pizzo Mondello (Sicily) and correlation to the Late Triassic Newark astrochronological polarity time scale. *Geol. Soc. Am. Bull.* **116**, 1043–1058. (doi:10.1130/B25326.1)
77. Rigo M, Trotter JA, Preto N, Williams IS. 2012 Oxygen isotopic evidence for Late Triassic monsoonal upwelling in the northwestern Tethys. *Geology* **40**, 515–518. (doi:10.1130/G32792.1)
78. Sun YD, Orchard MJ, Kocsis ÁT, Joachimski MM. 2020 Carnian–Norian (Late Triassic) climate change: evidence from conodont oxygen isotope thermometry with implications for reef development and Wrangellian tectonics. *Earth Planet. Sci. Lett.* **534**, 116082.
79. Purnell MA. 1994 Skeletal ontogeny and feeding mechanisms in conodonts. *Lethaia* **27**, 129–138. (doi:10.1111/j.1502-3931.1994.tb01567.x)
80. Hogancamp NJ, Barrick JE, Strauss RE. 2016 Geometric morphometric analysis and taxonomic revision of the Gzhelian (Late Pennsylvanian) conodont *Idiognathodus simulator* from North America. *Acta Palaeontologica Polonica* **61**, 477–502. (doi:10.4202/app.00198.2015)
81. Jones DO, Purnell MA. 2006 A new semi-automatic morphometric protocol for conodonts and a preliminary taxonomic application. In *Automated object identification in systematics: theory, approaches, and applications* (ed. N Macleod), pp. 239–259. Boca Raton, FL: CRC Press.
82. Rohlf FJ. 2010 *Tpsdig v2. 16. Department of ecology and evolution*. Stony Brook, NY: State University of New York.
83. Rohlf FJ. 2010 *Tpsrelw, relative warps analysis. Department of ecology and evolution*. Stony Brook, NY: State University of New York at Stony Brook.
84. Harper WV. 2016 Reduced major axis regression. In *Wiley StatsRef: statistics reference online* (eds N Balakrishnan, T Colton, B Everitt, W Piegorsch, F Ruggeri, JL Teugels). See https://onlinelibrary.wiley.com/doi/abs/10.1002/9781118445112.stat07912.
85. Klingenberg CP. 2011 MorphoJ: an integrated software package for geometric morphometrics. *Mol. Ecol. Resour.* **11**, 353–357. (doi:10.1111/j.1755-0998.2010.02924.x)
86. Souquet L, Guenser P, Girard C, Mazza M, Rigo M, Goudemand N. 2022 Data from: Temperature-driven heterochrony as a main evolutionary response to climate changes in conodonts. Figshare. (doi:10.6084/m9.figshare.c.6238496)